

cold, 70- to 80-km-thick mantle lid (Fig. 6). This would suggest a history where the range lay at about 4000 to 5500 m, and then subsided to 2000 to 3000 m as a result of extension (32).

REFERENCES AND NOTES

1. W. J. Zhao *et al.*, *Nature* **366**, 557 (1993); G. Zandt, A. A. Velasco, S. L. Beck, *Geology* **22**, 1003 (1994).
2. Assuming isostatic equilibrium, a change Δh in the thickness of any given layer in the lithosphere results in elevation change $\Delta e = \Delta h (\rho_a - \rho_e) / \rho_a$ where ρ_a is the density of the layer. Here we assume that $\rho_a = 3250 \text{ kg/m}^3$ and the average density of the crust is 2800 kg/m^3 .
3. *The New York Times Atlas of the World* (Random House, New York, ed. 4, 1994); in this paper, elevation refers to regionally averaged elevations [for example, W. H. Diment and T. C. Urban, *U.S. Geol. Surv. Geophys. Invest. Map, GP-933* (1981)], which may be considered isostatically compensated.
4. B. Wernicke, in *The Geology of North America*, B. C. Burchfiel, P. W. Lipman, M. L. Zoback, Eds. (The Geological Society of America, Boulder, CO, 1992), vol. G-3, chap. 12.
5. J. P. Eaton, *Calif. Div. Mines Geol. Bull.* **190**, 419 (1966); L. C. Pakiser and J. N. Brune, *Science* **210**, 1088 (1980); W. D. Mooney and C. S. Weaver, *Geol. Soc. Am. Mem.* **172**, 129 (1989); *P*-wave velocity of the root was suggested to be 6.9 km/s.
6. C. H. Jones, H. Kanamori, S. W. Roecker, *J. Geophys. Res.* **99**, 4567 (1994).
7. Arrays combine three broad-band (10- or 30-s period) and six to eight short-period seismometers in an L-shaped or linear array. Traces are summed into beams using a time-shift so that the teleseismic *P* arrives simultaneously on all traces, thus greatly reducing scattered and reflected energy.
8. F. Birch, *J. Geophys. Res.* **66**, 2199 (1961); W. J. Ludwig, J. E. Nafe, C. L. Drake, in *The Sea: Ideas and Observations on Progress in the Study of the Seas*, A. E. Maxwell, Ed. (Wiley Interscience, New York, 1970), vol. 4, pp. 53–84.
9. S. Ruppert and M. M. Fliedner, unpublished data.
10. Variations in *PmP* arrival times for the north-south profile indicate only a 2° northward dip on the Moho, consistent with analysis of fan shots (M. M. Fliedner and S. Ruppert, unpublished data), justifying neglect of three-dimensional effects for the purposes of this analysis.
11. D. S. Carder, *Bull. Seismol. Soc. Am.* **63**, 571 (1973).
12. D. H. Oppenheimer and J. P. Eaton, *J. Geophys. Res.* **89**, 10,267 (1984); W. S. Holbrook and W. D. Mooney, *Tectonophysics* **140**, 49 (1987).
13. J. F. Gibbs and J. C. Roller, *U. S. Geol. Surv. Prof. Pap.* **550-D** (1966), p. D125.
14. R. W. Groom and R. C. Bailey, *J. Geophys. Res.* **94**, 1913 (1989); J. T. Smith and J. R. Booker, *ibid.* **96**, 3905 (1991).
15. S. K. Park, B. Kirasuna, G. Jiracek, C. Smith, unpublished data.
16. E. B. Watson and J. M. Brennan, *Earth Planet. Sci. Lett.* **85**, 497 (1987).
17. T. J. Shankland, R. J. O'Connell, H. S. Waff, *Rev. Geophys. Space Phys.* **19**, 394 (1981).
18. F. C. Dodge, L. C. Calk, R. W. Kistler, *J. Petrol.* **27**, 1277 (1986).
19. F. C. Dodge, J. P. Lockwood, L. C. Calk, *Geol. Soc. Am. Bull.* **100**, 938 (1988); B. Mukhopadhyay, thesis, University of Texas at Dallas (1989); B. Mukhopadhyay and W. I. Manton, *J. Petrol.* **35**, 1417 (1994).
20. Trace element investigations (M. N. Ducea, R. W. Kistler, J. B. Saleeby, unpublished data) rule out any link with the host volcanic rocks.
21. Mineral rim compositions of 31 CS and HS samples displaying textural equilibrium were determined using the Caltech JEOL 733 electron microprobe. Geobarometers used included net-transfer reactions such as Al-in-orthopyroxene co-existing with garnet [S. L. Harley and D. H. Green, *Nature* **300**, 697 (1984)], while geothermometers involved mainly Fe-Mg exchange reactions [for example, R. Powell, *J. Metamorphic Geol.* **3**, 231 (1985)].
22. A. H. Lachenbruch, *J. Geophys. Res.* **73**, 6977 (1968); R. W. Saltus and A. H. Lachenbruch, *Tectonics* **10**, 325 (1991).
23. Basaltic Volcanism Study Project, *Basaltic Volcanism in the Terrestrial Planets* (Pergamon, New York, 1981).
24. B. Wernicke, *Can. J. Earth Sci.* **22**, 108 (1985); C. H. Jones, *Tectonics* **6**, 449 (1987); C. H. Jones *et al.*, *Tectonophysics* **213**, 57 (1992).
25. B. C. Burchfiel, D. S. Cowan, G. A. Davis, in *The Geology of North America*, B. C. Burchfiel, P. W. Lipman, M. L. Zoback, Eds. (The Geological Society of America, Boulder, CO, 1992), vol. G-3, chap. 8.
26. Two domains of extreme upper crustal extension (>300%) are interspersed with little-extended areas (<10 to 15%) that include parts of the Basin and Range, Sierra Nevada, and Colorado Plateau [Fig. 1; B. Wernicke, G. J. Axen, J. K. Snow, *Geol. Soc. Am. Bull.* **100**, 1738 (1988)]. Downward extrapolation of extension through the entire crust results in an improbable reconstruction, with 90- to 100-km-thick crust interposed with areas of 35-km-thick crust. Fluid behavior of the deep crust across the region, such that it is hydraulically pumped toward areas of upper crustal extension [for example, B. Wernicke, in *Exposed Cross Sections of the Continental Crust*, M. Salisbury and D. Fountain, Eds. (Kluwer, Dordrecht, Netherlands, 1990), pp. 509–544] results in a relatively flat reconstructed Moho (Fig. 6).
27. M. N. Christensen, *Geol. Soc. Am. Bull.* **76**, 1105 (1966); J. R. Unruh, *ibid.* **103**, 1395 (1991); N. K. Huber, *U. S. Geol. Survey Prof. Pap.* **1197** (1981); D. I. Axelrod, *Univ. Calif. Publ. Geol. Sci.* **121** (1980); T. A. Dumitru, *J. Geophys. Res.* **95**, 4925 (1990).
28. S. T. Crough and G. A. Thompson, *Geology* **5**, 396 (1977); G. A. Thompson and M. L. Zoback, *Tectonophysics* **61**, 149 (1979).
29. J. Polet and D. L. Anderson, *Geology* **23**, 205 (1995).
30. S. I. Akimoto, *Tectonophysics* **13**, 167 (1972); T. H. Jordan, in *The Mantle Sample*, F. R. Boyd and H. O. A. Meyer, Eds. (American Geophysical Union, Washington, DC, 1979), vol. 2, pp. 1–14.
31. C. E. Forest, P. Molnar, K. A. Emanuel, *Nature* **374**, 347 (1995); E. E. Small and R. S. Anderson, *Science* **270**, 277 (1995).
32. We assume that the mean crustal density is 2700 to 2800 kg/m³ and use calculations of A. H. Lachenbruch and P. M. Morgan [*Tectonophysics* **174**, 39 (1990)].
33. Supported by the Continental Dynamics Program of the National Science Foundation (EAR-9120690 to S.P., EAR-9120688 to G.J., EAR-9119263 to P.M., and EAR-9120689 to R.P.), the Department of Energy (DE-FG03-93ER14311 to R.C.), the U.S. Navy (China Lake Naval Weapons Center), and the U.S. Air Force (Office of Scientific Research). Key logistical support was provided by the National Park Service, Bureau of Land Management, and U.S. Forest Service.

30 August 1995; accepted 14 November 1995

Fluorination of Diamond Surfaces by Irradiation of Perfluorinated Alkyl Iodides

V. S. Smentkowski and John T. Yates Jr.*

A facile method for chemically functionalizing diamond surfaces has been developed using x-ray irradiation of perfluoroalkyl iodide layers on the surface. Perfluoroalkyl radicals chemically bond to the diamond surface and can be thermally decomposed to produce strongly bound surface C–F bonds that are stable at high temperatures.

Diamond film coatings can significantly improve the surface properties of many materials in applications such as cutting tools, biological implants, optical disks, lenses, and windows (1). In each of these applications, it may be desirable to modify the properties of the outer surface of the diamond film itself to produce special surface properties. The chemical modification of diamond surfaces is one route for producing useful surface properties. One modifier that offers promise for the improvement of the behavior of diamond surfaces is fluorine (2); the strong C–F bonds of fluorine (3) on diamond surfaces provide enhanced lubricity (4) and enhanced stability under oxidizing conditions at elevated temperatures (5).

Until now, diamond surfaces have been fluorinated only with extreme methods involving molecular F₂ (5), atomic F (6), XeF₂ (4, 7), and fluorine-containing plasmas (8). Each of these surface-modification methods involves the handling of corrosive gases under harsh treatment conditions. In addition,

only partial fluorination of the diamond surfaces studied was achieved with these extreme methods (4–8). A recent, extensive review showed that the attachment of long chain fluoroalkyl species directly to diamond surfaces has not been reported (9), although attachment of such species by silylation on oxidized diamond is known (10).

We present a method for the deposition of more than one F atom per surface C atom on diamond. The fluorinated alkyl layer achieved by this method decomposes between 300 and 700 K to produce a highly stable form of chemisorbed fluorine on the diamond surface that then thermally decomposes over a wide temperature range up to 1500 K (11).

Perfluorinated alkyl iodides (C_xF_{2x+1}I) were used as a source of radiation-produced perfluorinated alkyl radicals that attack the diamond surface and anchor themselves there. Irradiation with x-rays dissociated the weak C–I bond (3, 12) in both C₄F₉I and CF₃I layers condensed on a diamond (100) single crystal (11). The x-ray irradiation was used also for x-ray photoelectron spectroscopy (XPS) measurements of the nature of the surface layer. The diamond

Surface Science Center, Department of Chemistry, University of Pittsburgh, Pittsburgh, PA 15260, USA.

*To whom correspondence should be addressed.

(100) surface was first cleaned by heating the surface to 1450 K in an ultrahigh vacuum (13), a procedure that removes surface impurities, including surface-bound hydrogen, and results in a graphite-free surface (14). The XPS measurement of the C(1s), I(3d), and F(1s) regions of the spectrum of a thick layer of C₄F₉I condensed on the clean diamond(100) surface at 119 K is shown at the top of Fig. 1. Spectral features characteristic of the condensed C₄F₉I layer were observed, and the underlying emission from the diamond C(1s) level at a binding energy of 284.0 eV (14) was almost completely suppressed by the thick overlayer.

Subsequent x-ray excitation (MgK α ,

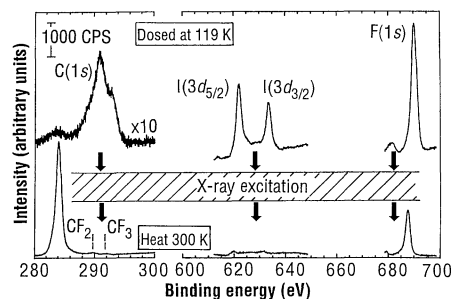


Fig. 1. XPS spectra of a C₄F₉I condensed overlayer on diamond(100) at 119 K (top) and the same overlayer after 180 min of x-ray irradiation at 119 K and heating to 300 K to desorb nondecomposed C₄F₉I (bottom). The C₄F₉I exposure was 5×10^{16} cm⁻² in this and subsequent figures. The presence of adsorbed CF₃(CF₂)₃ species and surface I species is indicated. The top C(1s) spectrum is multiplied by a factor of 10 for clarity. Intensity is measured in counts per second (CPS).

1253.6 eV, 300 W, 180 min) and then heating to 300 K to desorb nondecomposed C₄F₉I revealed the presence of chemically bound surface fluorine and surface iodine in addition to the C(1s) emission from the diamond substrate. Two additional C(1s) features characteristic of CF₂ and CF₃ groups (8, 15) were evident at 289.7 and

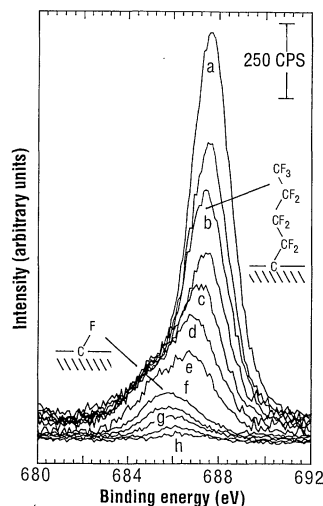


Fig. 3. A series of XPS spectra of the F(1s) region showing features due to C₄F₉- groups that decompose thermally to produce surface C-F groups that cover the diamond(100) surface. (The schematic location of the anchored C₄F₉- group and the surface C-F bonds are noted on the figure.) The surface C-F groups have an initial coverage of ~ 0.6 F/surface C atom at 700 K and remain on the surface to 1500 K; a, 300 K; b, 404 K; c, 500 K; d, 600 K; e, 850 K; f, 950 K; g, 1150 K; and h, 1500 K.

291.9 eV, respectively (Fig. 1, bottom), and were attributed to the CF₂ and CF₃ groups in the adsorbed CF₃(CF₂)₃- species on the diamond surface. The relative C(1s) binding energies were in excellent agreement with ab initio calculations (11). The ratio of the C(1s) integrated intensities in the two features was 2.8 ± 0.1 , as expected for this species if self-screening effects are essentially absent. The F(1s) yield from the anchored C₄F₉- groups (measured after the desorption of excess C₄F₉I by heating to 300 K) increased monotonically from zero to a plateau over the 180-min irradiation period, showing that the production of the C₄F₉- groups was radiation-induced (11). The ratio of the two C(1s) intensities remained approximately constant as the C₄F₉- groups decomposed in ultrahigh vacuum at temperatures above 300 K (Fig. 2).

The F(1s) intensity was also monitored during the thermal decomposition of the C₄F₉- groups on the diamond surface (Fig. 3). At least two F(1s) features were observed. At an F(1s) binding energy near 687.6 eV, we observed F(1s) emission characteristic of both the CF₂ and CF₃ groups of the anchored C₄F₉- species. At 950 K, all evidence for these XPS features had disappeared, and an F(1s) emission feature near 686 eV remained. This F(1s) feature at lower binding energy was due to C-F bonds on the diamond surface. The magnitude of the shift to lower binding energy agreed well with ab initio calculations (11). This chemisorbed surface fluorine persisted up to ~ 1500 K.

The various stages of the thermal de-

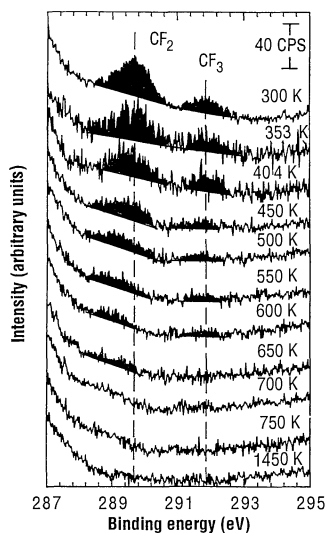


Fig. 2. A series of XPS spectra of the C(1s) region showing features attributed to CF₃ and CF₂ moieties in adsorbed CF₃(CF₂)₃- groups anchored on diamond(100). The thermal decomposition of the C₄F₉- groups was monitored after the surface was heated in an ultrahigh vacuum to the temperatures indicated.

Fig. 4. Intensity of XPS features as a function of heating fluorinated diamond(100) in an ultrahigh vacuum. Below 300 K, undecomposed C₄F₉I desorbs. In the temperature range from 300 to ~ 900 K, C₄F₉- groups thermally decompose to produce adsorbed F species on the diamond surface. These surface C-F groups thermally decompose in the range from ~ 900 to 1500 K. The decrease in F(1s) intensity is shown in two stages. In the second stage (above 900 K), the data points on the second F(1s) curve are intensity $\times 10$.

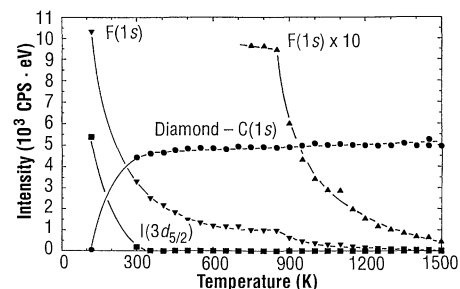
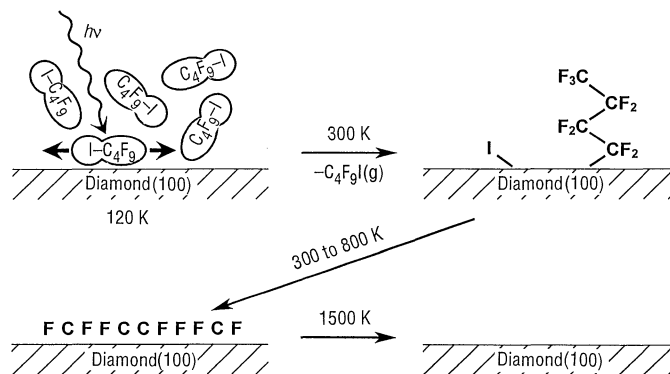


Fig. 5. The stages of fluorination and decomposition of fluorinated diamond surfaces.



composition of C_4F_9I on diamond(100) are shown in Fig. 4. Here the initial desorption of C_4F_9I upon heating from 119 to 300 K can be seen from the behavior of the F(1s), I(3d), and diamond C(1s) features. The first stage of the decrease in F(1s) integrated intensity, due to the loss of chemically bound fluorine, occurred slowly in the temperature range from 300 to 900 K as C_4F_9- species thermally decomposed to produce C-F bonds on the diamond surface (compare with Figs. 2 and 3). The second stage of F(1s) depletion was observed at temperatures above about 900 K as surface-bound fluorine was removed. The stability of the chemisorbed diamond surface C-F bonds produced from anchored C_4F_9- species was similar or superior to the behavior for similar C-F groups produced by direct fluorination with F atoms (6).

The coverage of fluorine on diamond(100) has been estimated using C(1s) and F(1s) intensities from clean and fluorinated diamond, respectively (11). An electron mean free path of $\lambda = 14 \text{ \AA}$ (16) for C(1s) electrons and XPS relative sensitivity factors of $S_C = 0.2$ and $S_F = 1.0$ (17) were used. For the anchored C_4F_9- layer produced by heating to 300 K after x-ray irradiation of the C_4F_9I layer, N_F/N_C was equal to 2.0, where N_C is the number of surface C atoms on the clean diamond surface, and N_F is the number of surface F atoms in the anchored C_4F_9- species. When the C_4F_9- species were decomposed almost completely near 700 K, N_F/N_C equaled 0.6 for a single experiment. Similar experiments with CF_3I only yielded N_F/N_C of ~ 0.2 at 300 K. Thus, the use of a longer chain perfluoroalkyl iodide drives the fluorination of diamond surfaces to higher levels.

The experiments described above were carried out on atomically clean diamond surfaces to study the inherent reactivity of the diamond surface. However, diamond surfaces are passivated by the presence of surface C-H bonds (9), and this passivation would be expected to make the method described above impractical in most technological cases because of the need for high-temperature treatment of the passivated diamond to remove surface hydrogen before fluorination. We repeated the fluorination experiments on a deuterium-passivated diamond(100) surface and found evidence for the production of DI species at 119 K and for the subsequent fluorination of the diamond(100) surface (11). Apparently, the free radical species produced by radiation-induced decomposition of the C-I bond in C_4F_9I molecules are able to abstract D atoms from C-D bonds on the diamond surface to form DI and to facilitate attachment of C_4F_9- groups to the diamond surface (11). This observation indicates that the radiation-induced fluorination of hydrogen-terminated diamond surfaces that

are technologically useful can be achieved by the methods described above.

The radiation-induced mechanism for the fluorination of diamond was not investigated in this work. A variety of radiation-induced processes could be responsible, including direct photoionization by x-rays and electron-stimulated dissociation (18) due to secondary electron emission from the irradiated substrate. Stray electrons produced in the x-ray source are not responsible for this effect (11). It is well known that the weak C-I bond in C_4F_9I (bond energy = 2.05 eV) (3, 12) can be easily photolyzed, and this route is commonly used to induce free radical chemistry in homogeneous phase (19). In the stages of fluorination and decomposition of fluorinated diamond surfaces (Fig. 5), C-I bond scission at 120 K, followed by radical attachment to the diamond surface, precedes the thermal decomposition of anchored C_4F_9- groups to yield F atoms that are chemically bonded to the diamond surface.

REFERENCES AND NOTES

1. P. K. Bachmann and R. Messier, *Chem. Eng. News* **67** (no. 20), 24 (15 May 1989); J. E. Field, *The Properties of Diamonds* (Academic Press, New York, 1979); *The Properties of Natural and Synthetic Diamonds* (Academic Press, New York, 1992); R. Pool, *Science* **249**, 27 (1990); B. J. Feder, *New York Times*, 21 February 1990, p. C4; D. E. Koshland Jr., *Science* **250**, 1637 (1990).
2. S. K. Ritter, *Chem. Eng. News* **73** (no. 9), 39 (27 February 1995); K. E. Spear, *J. Am. Ceram. Soc.* **72**, 171 (1989).
3. R. Weast, Ed., *Handbook of Chemistry and Physics* (CRC Press, Boca Raton, FL, ed. 63, 1982), p. F-199.
4. D. S. Y. Hsu and N. H. Turner, paper presented at Fourth SDIO/First Office of Naval Research Diamond Technology Initiative Symposium, Arlington, VA, 11 to 13 July 1989.
5. D. E. Patterson, R. H. Hauge, J. L. Margrave, *Mater. Res. Soc. Symp. Proc.* **140**, 351 (1989).
6. A. Freedman and C. D. Stinespring, *Appl. Phys. Lett.* **57**, 1194 (1990); *Mater. Res. Soc. Symp. Proc.* **204**, 571 (1991); *Proc. Electrochem. Soc.* **91**, 494 (1991); *New Diamond Sci. Technol. Proc. Int. Conf.* **2**, 321 (1991).
7. J. F. Morar *et al.*, *Phys. Rev. B* **33**, 1340 (1986); J. F. Morar *et al.*, *ibid.*, p. 1346.
8. P. Cadman, J. D. Scott, J. M. Thomas, *J. Chem. Soc. Chem. Commun.* **1975**, 654 (1975).
9. J. Wei, V. S. Smentkowski, J. T. Yates Jr., *Critical Reviews in Surface Chemistry* (CRC Press, Boca Raton, FL, in press).
10. A. Katz, S. P. Murarka, Y. I. Nissim, J. M. E. Harper, *Mater. Res. Soc. Symp. Proc.* **260**, 905 (1992).
11. V. S. Smentkowski, J. T. Yates Jr., X. Chen, W. A. Goddard III, in preparation.
12. E. N. Okafu and E. Whittle, *Int. J. Chem. Kinetics* **7**, 287 (1975).
13. V. S. Smentkowski and J. T. Yates Jr., *J. Vac. Sci. Technol. A* **11**, 3002 (1993).
14. V. S. Smentkowski, H. J. Jänsch, M. A. Henderson, J. T. Yates Jr., *Surf. Sci.* **330**, 207 (1995).
15. P. Cadman, J. D. Scott, J. M. Thomas, *Surf. Interface Anal.* **1**, 115 (1979).
16. B. B. Pate, *Surf. Sci.* **165**, 83 (1986); S. Evans, R. G. Pritchard, J. M. Thomas, *J. Phys. C* **10**, 2483 (1977).
17. *Empirical Atomic Sensitivity Factors for MgK α Irradiation* (Leybold Vacuum Products, Cologne, Germany, 1984); C. D. Wagner, W. M. Riggs, L. E. Davis, J. F. Moulder, G. E. Muilenberg, *Handbook of X-Ray Photoelectron Spectroscopy* (Perkin-Elmer, Eden Prairie, MN, 1979).
18. R. D. Ramsier and J. T. Yates Jr., *Surf. Sci. Rep.* **12**, 243 (1991).
19. H. Okabe, *Photochemistry of Small Molecules* (Wiley, New York, 1978).
20. We thank the Air Force Office of Scientific Research for support of this work (contract F49620-92-J-0192).

27 June 1995; accepted 23 October 1995

Functional Evidence for Indirect Recognition of G·U in tRNA^{Ala} by Alanyl-tRNA Synthetase

K. Gabriel, Jay Schneider, William H. McClain*

The structural features of the G·U wobble pair in *Escherichia coli* alanine transfer RNA (tRNA^{Ala}) that are associated with aminoacylation by alanyl-tRNA synthetase (AlaRS) were investigated in vivo for wild-type tRNA^{Ala} and mutant tRNAs with G·U substitutions. tRNA^{Ala} with G·U, C·A, or G·A gave similar amounts of charged tRNA^{Ala} and supported viability of *E. coli* lacking chromosomal tRNA^{Ala} genes. tRNA^{Ala} with G·C was inactive. Recognition of G·U by AlaRS thus requires more than the functional groups on G·U in a regular helix and may involve detection of a helical distortion.

RNA-protein interactions require the stable merging of two complementary tertiary structures. The G·U wobble base pair at positions 3 and 70 (3·10) of the acceptor helix in *E. coli* tRNA^{Ala} is a major determinant of the interaction of this RNA with AlaRS during aminoacylation (1). The

prevalent direct recognition hypothesis states that AlaRS interacts directly with functional groups of the G·U pair in the minor groove of an A-form helix (2). An alternative indirect recognition hypothesis states that AlaRS recognition of G·U in tRNA^{Ala} depends on a local helical distortion promoted by G·U as well as on recognition of its functional groups (3). To distinguish between these hypotheses, we tested the in vivo aminoacylation capacity of

Department of Bacteriology, University of Wisconsin, Madison, WI 53706, USA.

*To whom correspondence should be addressed.